

Determination of Coefficient of Skin Frictions for Riblet and Smooth Plate Models

Julius Thaddeus

Abstract - Drag reduction in wall-bounded flows can be achieved by the passive flow control technique, riblets. In this article, two model flat surfaces, smooth and riblet were investigated using hot wire anemometry method to determine their coefficient of skin frictions and hence, possible drag reductions. The results obtained indicate that the riblet flat plate model had coefficient of skin friction $C_f = 0.0056$ while the smooth one had $C_f = 0.0059$. These results indicates that 5.1% drag reduction can be achieved from the application of riblets technology in wall-bounded flows.

Keywords: Turbulence, drag reduction, riblets, smooth, boundary layers, skin friction

1. INTRODUCTION

In recent years, drag reduction in turbulent boundary layer has become an important area of fluid dynamics research. Specifically, rising costs of fuel greatly emphasized the usefulness and necessity of developing efficient viscous drag reduction methods. The impetus for turbulent drag reduction research is both tremendous and obvious as large proportion of the energy expenditure for all types of transportation (air, sea, land) and for many industrial and propulsion processes is simply to overcome turbulent skin friction. The payoff from invention and development of successful approaches can conservatively be estimated in billions, irrespective of which country's currency one considers. Riblets as a passive method, installed over a smooth surface in the turbulent boundary layer, can reduce drag by approximately 6-8% in turbulent flow. The advantages of using riblets, as a type of micro-structured surfaces in many engineering applications have been realized. For instance, the flight testing of aircrafts with ribleted structural surfaces by Boeing [1], Airbus [2], and NASA [3] demonstrated the important effects of riblets. Sareen [4] also employed different sizes of sawtooth riblets applied to the DU 96-W-180 air foil for a wind turbine. Apart from the aeronautical applications as shown in figure 2 below, other industrial uses for riblets have been identified and in particular, biological surfaces with geometrically complex micro-featured surfaces [5].

The approaches of research choice prior to the late 1970s involved either laminar flow control (LFC), which had fairly severe limitations as to application (surface finish/unit Reynolds number, disturbance environment, etc.), or techniques to alter the average flow/drag directly

such as wetted area minimization, reduced roughness, use of a "Stratford closure" (adverse pressure gradient), mass injection, and bubbles to reduce the average near-wall density in water, [6]. An exception was the use of polymers to affect, in an unknown manner, the turbulence field directly. Following an unsuccessful four-year campaign to apply "complaint walls" to the case of airflow (1972-1976) [7], and recognizing the extensive contemporary research on wall turbulence structure, the NASA Langley drag-reduction effort turned toward a more overt invention-orientated mode of operation in 1976 and posed the following question: Does a smooth flat surface really provide the lowest net drag or are there other (nonplanar) surfaces which could interfere with various facets of the wall turbulence structure and provide a net drag reduction? By 1978 two new approaches had arisen from this effort: (a) riblets, and (b) large-eddy breakup devices, [8]. the latter was developed in cooperation with the IIT group (H. Nagib) under grant. Along with these two approaches, which are still the current "front runners" among the passive, nonplanar techniques, many other approaches were tried and discarded.

This study, therefore, explores concept for control of turbulent boundary layers leading to skin friction reduction by comparing two model surfaces (riblet and smooth).

2. METHODOLOGY

This study pertains to the measurement technique for deriving the skin friction inside a wind tunnel over smooth and ribleted surfaces. Recently derived measurements of good quality, using pitot tubes, 5 micron single hot-wire

and automated transverse, were used to assess critically, and then to improve the experimental accuracy of , the empirical coefficient as well as the determination of the surface shear and skin friction. Each sensor was calibrated in free-stream flow before and after each profile or each set of data points was measured. If these two calibrations were in disagreement by more than 2-3%, or if the error was more than 0.01, the entire process was repeated.

The experiment was conducted on the vertical blower wind tunnel at Brunel University London, as shown in figure 1 and the dimensions of the test section was 150mm x 50mm. This tunnel also had a filter at inlet to remove dust and dirt particles in order to minimize hot-wire contamination and breakage. In addition, sandpaper was used to trigger artificially the boundary layer into being turbulent, which occurred on the plates at zero angle of incident. This is often referred to as a canonical zero-pressure turbulent gradient boundary layer.

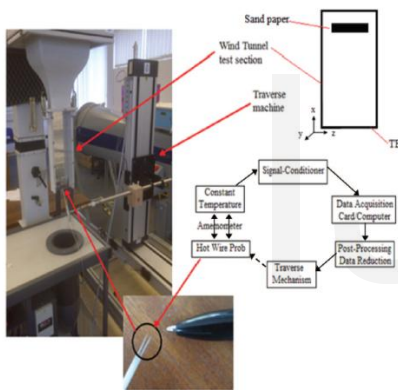


Figure 1. Experimental testing setup by using wind tunnel and hot-wires data logging system

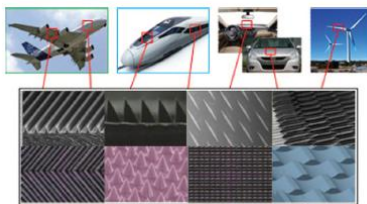


Figure 2. Typical micro-structured surfaces and their engineering application [9]

The measurements were taken using an automated transverse in the vertical (y), streamwise (x) and spanwise (z) directions, with a displacement accuracy of 0.01mm, 0.01mm and 0.1mm respectively. The transverse machine

allows 3-D placement of measurement probes, which can position a thermal probe or pitot tube at any (x,y,z) position and is controlled by the stepper motor, which uses the thermalpro software on the computer.

The signal from the single hot wire were acquired at 20kHz, after passing through a 10kHz anti-aliasing filter and the digitized voltage from the hot wire was then converted to velocity by interpolating the 4th- order polynomial velocity-voltage calibration curve, (6). Voltages were acquired using a National Instrument Data Acquisition DaqBoard/3005 card, which consisted of a 1-MHz A/D with 16-bit resolution.

The collected data from the acquisition card in the first step was reduced by Thermalpro. Next, the mean and root mean square (rms) of the velocity data for the velocity profiles were calculated as:

$$U_{mean} = \frac{1}{N} \sum_{i=1}^N U_i \dots\dots\dots (1)$$

$$U_{rms} = \sqrt{\frac{1}{N} \sum_{i=1}^N (U_i - U_{mean})^2} \dots\dots\dots (2)$$

Where N is the total number of samples in the velocity time series and the rms is the measure of the amount of deviation of a signal piece of data from its mean value, which is computed as the square root of the variance.

Furthermore, according to the log-law, the boundary layer profile was generated theoretically as follow:

$$\frac{u}{u_\tau} = \frac{1}{0.41} * \ln \left(\frac{y * u_\tau}{\nu} \right) + 5 \dots\dots\dots (3)$$

For non-dimensional velocity U^+

$$U^+ = \frac{u}{u_\tau} = \frac{u}{u_e} * \frac{u_e}{u_\tau} \dots\dots\dots (4)$$

$$y^+ = y * \frac{u_\tau}{\nu} \dots\dots\dots (5)$$

Where ν the kinematic viscosity of the air is, u_τ is the friction velocity, 0.41 is the Von Karman constant. u_e is the velocity at the edge of the boundary layer.

According to the formula, we substituted different values of friction velocity in order to fit the theoretical velocity and experimental velocity together so that we can get the skin friction coefficient number.

$$u_\tau = \sqrt{\frac{\tau_w}{\rho}} \dots\dots\dots (6)$$

$$C_f = \frac{\tau_w}{0.5 * \rho * u_e^2} \dots\dots\dots (7)$$

Finally, the skin friction coefficient number was obtained from equation (5) above. τ_w is the wall shear stress and ρ is the density of the air.

The schematic set up used for the experimental work was as shown below:



Figure 3. Schematic laboratory set-up for the experiment

3. RESULTS DISCUSSION

The modification of the onset of transition was achieved by careful analysis of the temporal signals of velocity (single hot-wire). This is, the freestream velocity at the inlet of the test section was measured at a distance of 22mm from the leading edge (U_∞) whilst at the outlet this velocity was measured at the edge of the plate. In addition, because of the effect of the side walls growing towards the leading edge, the inlet velocity was found to be 1.9% lower than that of outlet. Therefore, the free stream velocity measured at the middle of test section was used to normalise the data.

Figure 3 shows the mean velocity profile for the plate models.

In equations 6 & 7, the skin friction coefficient (C_f) and freestream velocities of the test section are given for the model surfaces. The method used to calculate C_f described in the next section. The skin friction coefficient $C_f = \frac{\tau_w}{0.5\rho U_\infty^2}$ increases with APG, which can be seen in figure 4 where C_f is presented for both smooth and riblet, and this increase is due to the decrease in the wall shear stress (τ_w).

The obtained results in figures 5 & 6 show the effect of riblets on decreasing skin friction and consequently drag. It can be seen that the skin friction on the ribleted plate has been reduced by 7% when compared to the smooth one.

The value of the skin friction coefficient C_f was determined by following a method similar to that of clausner [10]. For a given Mach number, Allen and Tudor [11] proposed a chart with a family of curves of $\frac{U}{U_\tau}$ versus $\frac{y U_\tau}{\nu}$ with C_f as the varying parameter. Using a single hot wire allows for measurements inside the buffer layer ($5 < y^+$ for size of riblet is in the range of the buffer layer, the clausner

chart can define local skin friction on both ribleted and smooth surfaces. By plotting the experimental profile on the chart, the skin friction coefficient was obtained by interpolating between the C_f curves.

The resulted polynomial equation for the velocity (m/s) conversion is:

$$y = 24.65x^4 - 111.51x^3 + 224.62x^2 - 226.37x + 90.164 \quad (6)$$

With variable x , as the voltage from the experimental data.

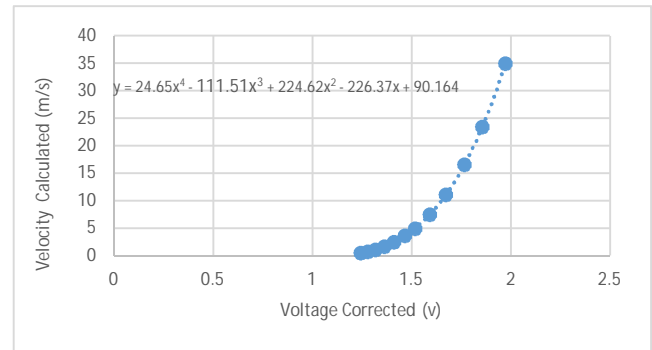


Figure 4. Velocity - Voltage Curve

At temperature $T = 18^\circ\text{C}$ (291K), from dry air property table:

Kinematic Viscosity $\nu = 1.487 \times 10^{-5} \text{ m}^2/\text{s}$, Air density $\rho = 1.216 \text{ kg/m}^3$

3.1 Smooth Plate:

From the law of wall: $\frac{U}{U_\tau} = \frac{1}{K} \ln\left(\frac{y U_\tau}{\nu}\right) + C$. Different values were substituted in order to find the best fit of the experimental data with the velocity profile plot of $U^+ \left(\frac{U}{U_\tau}\right)$ against $Y^+ \left(\frac{y U_\tau}{\nu}\right)$, and therefore, the best fit plot for the smooth surface plate was obtained when $U_\tau = 0.76$.

Where ν = Kinematic viscosity (m^2/s), U = Calculated (Converted) velocity (m/s), y = Distance of the probe away from the plate, U_τ = frictional velocity, $K = 0.41$ (constant) and $C = 5$ (Constant).

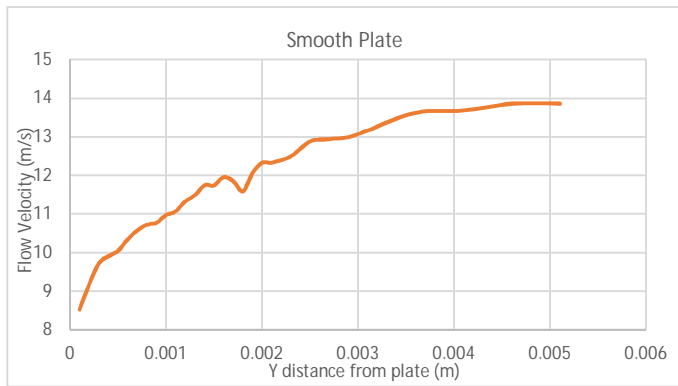


Figure 5. Boundary layer Velocity profile for Smooth Plate

The velocity at the edge of the boundary layer for the smooth surface plate, approximately $U_e = 14\text{m/s}$ was determined from figure 3 plot and hence, the wall shear stress was calculated thus:

$$\text{Wall shear stress } \tau_w = U_\tau^2 \times \rho = (0.76)^2 \times 1.216 = 0.702$$

$$\text{The coefficient of friction, } C_f = \frac{\tau_w}{0.5 \rho U_e^2} = \frac{0.702}{0.5 \times 1.216 \times 14^2} = 0.0059$$

Therefore, the coefficient of skin friction for the Smooth plate, $C_f = 0.0059$

The coefficient of skin friction for the smooth plate obtained above shows that the smooth plate has higher value and consequently higher drag force, as compare to that of riblet plate. This results from the fact that the flow layer close to the wall has less turbulence and hence more drag.

3.2 Riblet Plate:

On the other hand, from the law of wall: $\frac{U}{U_\tau} = \frac{1}{K} \ln\left(\frac{y U_\tau}{\nu}\right) + C$. Different values were substituted in order to find the best fit of the experimental data with the velocity profile plot of $U^+ \left(\frac{U}{U_\tau}\right)$ against $Y^+ \left(\frac{y U_\tau}{\nu}\right)$, and therefore, the best fit plot for the ribletted surface plate was obtained when $U_\tau = 0.80$.

Where ν = Kinematic viscosity (m^2/s), U = Calculated (Converted) velocity (m/s), y = Distance of the probe away from the plate, U_τ = frictional velocity, $K = 0.41$ (constant) and $C = 5$ (Constant).

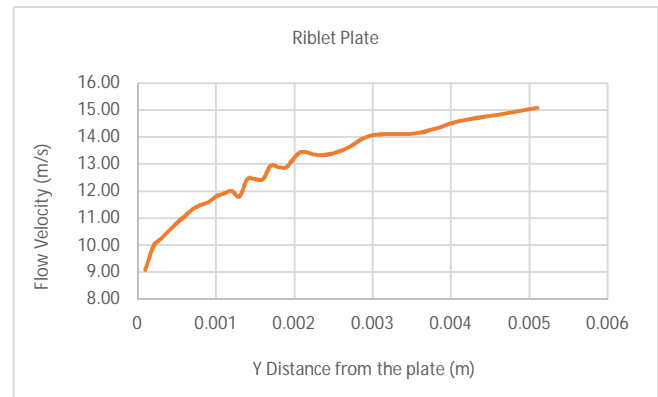


Figure 6. Boundary layer velocity profile for Riblet Plate

The velocity at the edge of the boundary layer for the riblet surface plate, approximately $U_e = 15\text{m/s}$ was determined from figure 6 plot and hence, the wall shear stress was calculated thus:

$$\text{Wall shear stress } \tau_w = U_\tau^2 \times \rho = (0.80)^2 \times 1.216 = 0.778$$

$$\text{The coefficient of friction, } C_f = \frac{\tau_w}{0.5 \rho U_e^2} = \frac{0.778}{0.5 \times 1.216 \times 15^2} = 0.0057$$

Therefore, the coefficient of friction for the Riblet plate, $C_f = 0.0057$

The coefficient skin friction for the riblet plate obtained above is lesser and consequently lesser drag force as compared to that of smooth plate. This drag reduction mechanism of the riblets is based on a hampering of the interaction of vortex structures in a turbulent flow close to the wall.

4. CONCLUSION

The experiment aimed at determining the coefficient of skin friction for smooth and riblet plates using hot-wire anemometry technique. The results obtained show that the coefficient of skin friction for smooth plate was obtained as $C_f = 0.0059$ and that of riblet plates as $C_f = 0.0056$. This laboratory experiment proved that ribletted surface can effect drag reduction by 5.1% when compared to smooth surface.

REFERENCES

1. McLean JD, Georg-Falvy DN and Sullivan P. Flight test of turbulent skin friction reduction by riblets. In: Conference on turbulent Drag Reduction by

- Passive means, The Royal Aeronautical Society, London, 15-17 September 1987, pp. 408-48.
2. Coustols E and Savill AM. Turbulent skin-friction drag reduction by active and passive means, AGARD, Report 786 part 1, Seine, France, 1992, pp.8.1-8.53.
3. Walsh MJ, Seller WL and McGinley CB. Riblets drag at flight conditions. J Aircraft 1989; 26(6): 570-575.
4. Sareen A. Drag reduction using riblet film applied to airfoil for wind turbines. PhD Thesis, University of Illinois at Urbana-Champaign, USA, 2012.
5. Itoh M, Tamano S, Iguchi R, Yokota K, Akino N, Hino R and Kubo S. Turbulent drag reduction by the seal fur surface. Phys. Fluids 2006; 18 (6): 065102.
6. Bushnell, D.M." Turbulent Drag Reduction for External Flows." Aircraft Drag Prediction and Reduction, AGARD Report 723, 1985
7. Bushnell, D.M., Hefner, J.N and Ash, R.L. "Effect of compliant Wall Motion on Turbulent Boundary Layers." Special Course on Concepts for Drag Reduction, AGARD R-654, Mar 1977
8. Hefner, J.N, Weinstein, L.M, and Bushnell, D.M. "Large-Eddy Breakup Scheme for Turbulent Viscous Drag reduction." Viscous flow drag reduction, Progress in Astronautics and Aeronautics, 1980, Vol. 72, 110-127
9. Samira SayadSaravi, Kai Cheng, Tze Pei Chong and Alexandros Vathylakis, 2014. *Design of Serrate-Semi-Circular Riblets with Application to Skin Friction Reduction on Engineering Surfaces*. School of Engineering and Design, Brunel University Cleveland Road, Uxbridge, UB8 3PH.
10. Clauser FH. Turbulent Boundary Layers in Adverse Pressure Gradient. J. Aeronaut. Sc. 1954; 21:91-108
11. Allen JM, and Tudor DH. Charts for interpolation of Local Skin Friction from Experimental Turbulent Velocity Profiles. Technical report, tech. Rep. NASA SP-3048, 1969.
12. Samira SayadSaravi and Kai Cheng. "A Review of Drag Reduction by Riblets and Micro-Textures in the Turbulent Boundary Layers." European Sci. J. November 2013 edition vol.9, No. 33 ISSN: 1857 – 7881.
13. S.P Wilkinson, J.B Anders, et all. "Turbulent Drag Reduction Research at NASA Langley: Progress and Plans." Int. J. Heat and Fluid Flow, Vol.9, No.3, September 1988.
14. Bushnell D.M, Hefner J.N and Ash R.L. "Effect of Compliant Wall Motion on Turbulent Boundary Layers." Special Course on Concepts for Drag Reduction. AGARD R-654, March 1977.
15. Qpedia 2007, "Advanced Thermal Solution Inc. 2007" Access online via: file:///C:/Users/user/Downloads/Qpedia_Dec07_Understanding%20hot%20wire%20anemometry.pdf
16. How to measure turbulence with hot-wire anemometer – *A practical guide*. By Finn E. Jorgensen 2002. Dantec Dynamics
17. Nick Hutchins, Kwing-So Choi, 2002. *Accurate measurements of local skin friction coefficient using hot-wire anemometry*. Elsevier Science Ltd, May-July 2002.

Julius Thaddaeus is currently a lecturer with Federal University Wukari, Nigeria. E-mail: Julius_manu@yahoo.com